Nuclear Engineering and Design 292 (2015) 213–221

Contents lists available at ScienceDirect

Nuclear Engineering and Design

journal homepage: www.elsevier.com/locate/nucengdes

DIONISIO 2.0: New version of the code for simulating a whole nuclear fuel rod under extended irradiation

Alejandro Soba*, Alicia Denis

Gerencia Ciclo del Combustible Nuclear, Comisión Nacional de Energía Atómica, Avenida General Paz 1499, 1650 San Martín, Provincia de Buenos Aires, Argentina

HIGHLIGHTS

- A new version of the DIONISIO code is developed.
- DIONISIO is devoted to simulating the behavior of a nuclear fuel rod in operation.
- The formerly two-dimensional simulation of a pellet-cladding segment is now extended to the whole rod length.
- An acceptable and more realistic agreement with experimental data is obtained.
- The prediction range of our code is extended up to average burnup of 60 MWd/kgU.

ARTICLE INFO

Article history:
Received 29 July 2014
Received in revised form 4 June 2015
Accepted 7 June 2015

E. Fuel engineering

ABSTRACT

The version 2.0 of the DIONISIO code, that incorporates diverse new aspects, has been recently developed. One of them is referred to the code architecture that allows taking into account the axial variation of the conditions external to the rod. With this purpose, the rod is divided into a number of axial segments. In each one the program considers the system formed by a pellet and the corresponding cladding portion and solves the numerous phenomena that take place under the local conditions of linear power and coolant temperature, which are given as input parameters. To do this a bi-dimensional domain in the r–z plane is considered where cylindrical symmetry and also symmetry with respect to the pellet mid-plane are assumed. The results obtained for this representative system are assumed valid for the complete segment. The program thus produces in each rod section the values of the temperature, stress, strain, among others as outputs, as functions of the local coordinates r and z. Then, the general rod parameters (internal rod pressure, amount of fission gas released, pellet stack elongation, etc.) are evaluated.

Moreover, new calculation tools designed to extend the application range of the code to high burnup, which were reported elsewhere, have also been incorporated to DIONISIO 2.0 in recent times.

With these improvements, the code results are compared with some 33 experiments compiled in the IFPE data base, that cover more than 380 fuel rods irradiated up to average burnup levels of 40–60 MWd/kgU. The results of these comparisons, which are presented here, reveal the good quality of the simulations.

© 2015 Elsevier B.V. All rights reserved.

1. Introduction

Simulation of a fuel rod is a complex problem that involves a large number of interconnected phenomena. The fuel performance codes need to adopt some simplifying hypotheses but without losing compatibility with the reality of the processes. In some codes, a one-dimensional (radial) representation of the rod is chosen, assuming cylindrical symmetry; to describe the whole rod, the same simulation procedure is performed at several axial nodes. These codes are often referred to as 1.5D. Examples of this calculation approach are TRANSURANUS (Lassmann, 1992), BACO (Marino et al., 1996a), ENIGMA (Palmer et al., 2000), FRAPCON (Geelhood et al., 2011), among others. FEMAXI makes an axis-symmetrical one-dimensional thermal analysis at several axial sections to obtain the temperature distribution in the entire rod; for the stress–strain problem this code performs a two-dimensional axis-symmetrical analysis to predict the local mechanical conditions between a pellet and its counterpart of cladding (PCMI) (Suzuki et al., 2013). FALCON performs a steady-state analysis using a stacked one-dimensional fuel rod representation, followed by a transient analysis using a

* Corresponding author. Tel.: +0054 11 4839 6796.
E-mail address: soba@cnea.gov.ar (A. Soba).

http://dx.doi.org/10.1016/j.nucengdes.2015.06.008
0029-5493/© 2015 Elsevier B.V. All rights reserved.

fully coupled two-dimensional *r–z* fuel rod representation (Zangari and Montgomery, 2004). The TOUTATIS code carries out 2D simulations of the rod and introduces several 3D subroutines to represent non-symmetric problems (Linet and Suo, 1993). The ALCYONE code performs a preliminary 1.5D simulation of the complete fuel rod to obtain information on the internal pressure and axial temperature distribution, among other parameters, and incorporates some 3D moduli to predict phenomena like hourglassing, relocation and cracking (Baurens et al., 2014). In the BISON code the fuel can be simulated either as a continuous smeared column or as discrete pellets, assuming 2D axysimmetric behavior. Some examples have been simulated using a 3D mesh, running the code in a supercomputer which contains over 12,000 processing cores (Williamson et al., 2012). This brief summary reveals how different the approaches to the rod behavior can be.

The fuel performance code DIONISIO is designed to describe most of the main phenomena occurring in a fuel rod during operation of the power reactor. A two dimensional domain consisting of a quarter of a longitudinal section of one pellet and the corresponding cladding segment is considered; cylindrical symmetry and also symmetry with respect to the pellet mid-plane are assumed to represent the rod volume associated to one pellet. The finite element method is used to integrate the non-linear thermal and mechanical differential equations (Soba and Denis, 2008a). Starting from a given (condensed) power history under normal operation conditions, the code version 1.0 predicts the temperature distribution in the domain, elastic and plastic stress and strain, creep, swelling and densification, release of noble gases, neodymium, caesium and iodine to the internal volume of the rod, gas mixing, pressure increase, irradiation growth of the Zircaloy cladding, development of an oxide layer on its surface and hydrogen uptake, restructuring and grain growth in the pellet. The effects of a corrosive atmosphere (SCC) either on the internal or external cladding wall as well as the possibility of pellet-cladding interaction (PCI) are also considered (Denis and Piotrkowski, 1996, 1997; Soba, 2007; Denis and Soba, 2003; Soba and Denis, 2006, 2008b). After performing these calculations in a single fuel pellet, the results are generalized to the rod length. This scheme implies the assumption that the linear power and the coolant temperature are uniform in the whole rod. Although a large number of properties are adequately simulated taking the average values of the input parameters, it is to be admitted that in certain instances this may lead to inaccurate prediction of some output variables. Initiation of fission gas release is an example of this limitation since the release surely starts at the middle of the rod, when the average linear power indicates that no release had to occur yet. At the opposite end, but for the same reasons, a simulation performed with the maximum of linear power would over-predict the amount of gas released and under-predict the time for initiation of release. It is worth mentioning that a correct simulation of gas release, both in regard to the start up instant as to the amount released is crucial for a correct simulation of the rest of the rod behavior since it affects the evolution of the internal pressure, the composition of the internal atmosphere in the rod, which thermal conductivity influences the temperature distribution, and in summary, all the physical parameters of the system.

In order to improve this code feature, the rod is divided into a user defined number of axial segments. Preliminary calculations give the coolant temperature and linear power distributions in terms of input parameters and axial coordinate, *z*. These functions provide the boundary conditions and the linear power for the whole rod. In each segment, with the boundary conditions assumed uniform and equal to the mean value in the segment, the program simulates the system formed by a pellet and the corresponding gap and cladding portions, as described above, and solves the numerous phenomena that take place under the local boundary conditions. The results obtained for this representative system are assumed to hold for the entire rod segment. Thus, in each segment the program produces as outputs the values of the temperature, stress, strain, gas release, among others, as functions of the local coordinates *r* and *z*. Then, the general rod parameters (internal rod pressure, gas inventory within the rod, pellet stack elongation, etc.) are evaluated at the end of every time step, combining the results of all the axial segments. This new code architecture, which constitutes one of the recent developments incorporated to the 2.0 version of DIONISIO, allows taking into account the axial variation of the linear power and coolant temperature and, consequently, evaluating the dependence of all the significant rod parameters with the longitudinal coordinate.

The new version of the code was also improved with the incorporation of calculation tools designed to extend the application range of the code to high burnup. On the one hand, a group of subroutines, which are tuned for UO_2 fuels in LWR conditions, predict the evolution of the radial distribution of ^{235}U, ^{236}U, ^{238}U, ^{239}Pu, ^{240}Pu, ^{241}Pu and ^{242}Pu (Soba et al., 2013). On the other hand, a set of subroutines has been included to simulate the microstructural modifications that the pellet suffers at its external edge under high and very high burnup conditions (Lemes, 2013). Furthermore, subroutines designed to predict the distribution of Caesium, Iodine, Neodymium and Xenon in the pellet solid lattice were also integrated to DIONISIO 2.0 (Soba et al., 2014), on the basis of experimental information reported in (Lassmann et al., 1995, 2003).

This paper is structured as follows: Section 2 is dedicated to describing the new features introduced in the code version 2.0; in Section 3 the more representative results obtained from the battery of experiments used in this work to test the code are described and analyzed; in Section 4 the general conclusions are summarized.

2. Description of the new features of the code

2.1. New domain of resolution

Fig. 1a shows a portion of a fuel rod consisting of several axial segments. The number of rod segments, and hence the number of pellets per segment, is defined by the user. All the pellets in a given segment are assumed to behave identically (subjected to identical boundary conditions) hence only one pellet, and the corresponding gap and cladding portions, need to be simulated in each segment. In every time step, a complete description of the local system variables is obtained by solving the tightly coupled non linear differential equations (heat, stress–strain, etc.) in such representative system, using the finite elements method. (In particular, the number of segments can be chosen equal to the number of pellets, in which case each pellet is individually described). Axial symmetry and also symmetry with respect to the transversal mid-plane of the pellet are assumed, as schematically shown in Fig. 1b. A typical finite elements discretization of the *r–z* domain is presented in Fig. 1c.

A simple model, described in detail elsewhere (Soba, 2007), has been chosen in DIONISIO to compute the coolant temperature axial profile, which input data are provided in the irradiation tests to be simulated. The linear power profile is also given in these tests (although in a variety of formats) or can be simply obtained from the experimental data. For the 2.0 code version, both profiles are discretized according to the user defined rod segmentation, to serve as input data for the separate simulations of the rod segments.

In the calculation scheme of DIONISIO 2.0, the 1.0 code version is run as many times as the number of segments in the rod. Then, the temperature and stress–strain distributions in the complete rod are obtained as step-like functions. With respect to the gas inventory, after calculating the amount of gas released by each

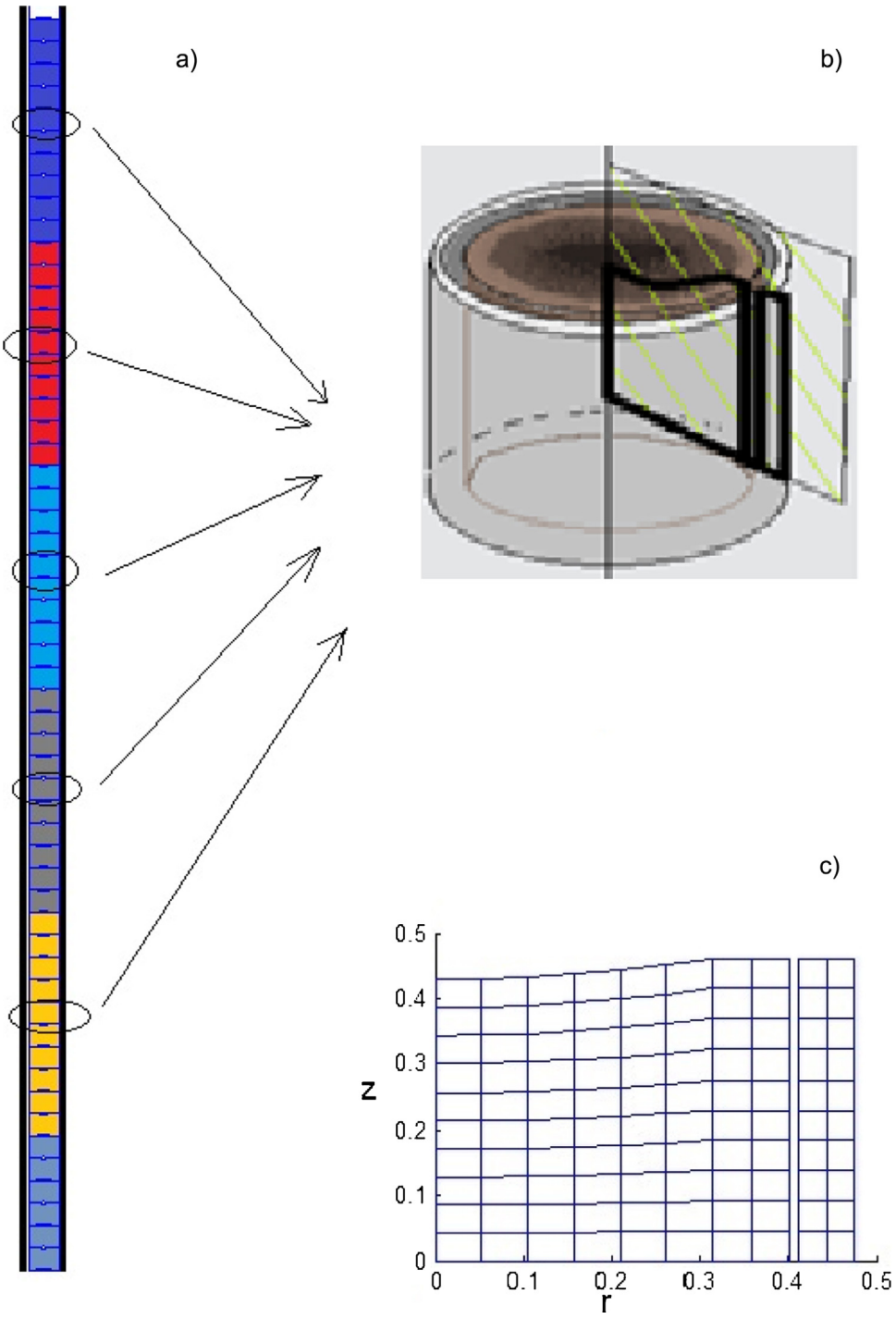

Fig. 1. (a) Portion of the rod formed by several segments, each one containing a number of pellets. (b) One pellet and the corresponding portions of gap and cladding; superimposed is the calculation domain. (c) Finite elements discretization of the domain.

rod segment (the release of one pellet times the number of pellets in the segment) the code evaluates the release of the whole rod. The composition of the gas mixture in the gap and its thermal conductivity (MATPRO Version 11, 1979) are recalculated in every time step. The internal rod pressure is evaluated with the ideal gas law using the total number of gas atoms in the free volume within the rod and the average temperature in the total void volume in the rod (gap and dishings in all the segments, and plenum). The elongations of every individual pellet and the corresponding cladding are added up to obtain the total elongation of the pellet stack and the rod.

The code has a parallel treatment of the linear solver using openMP (OpenMP, 2014). Parallelization by sectors using MPI (Message Passing Interface, 2015) is currently in progress.

2.2. High burnup considerations

2.2.1. Concentration of U and Pu isotopes

When the residence time of nuclear fuel rods of uranium oxide is increased beyond a given threshold value, several properties of the pellet material suffer changes and hence the subsequent behavior of the rod is significantly altered. Due to the absorption of

epithermal neutrons by ^{238}U (its absorption cross section exhibits resonant peaks in the energy range comprised between 5 and 2000 eV) and to the chains of nuclear reactions that take place thereafter, several Pu isotopes are born especially at the pellet periphery. In particular, the fissile character of ^{239}Pu and ^{241}Pu is the cause of the increased number of fission events that occur in that ring. For this reason, the radial dependence of the power generation rate and the burnup accumulation need to be considered. These parameters, which at low and intermediate burnup levels can be considered with a reasonably good approximation as uniformly distributed, reach values two or three times higher at the pellet edge than at the rest of the pellet when the average burnup exceeds a certain magnitude. The numerical codes designed to simulate fuel behavior under irradiation must include the radial distribution of power density, burnup and concentration of diverse nuclides to produce predictions valid in the high burnup range.

The complete treatment of all the isotopes involved in the nuclear reactions within the pellet in the whole energy spectrum is the task of the codes specialized in reactor physics. A simplified treatment consisting in reducing the energy spectrum to a single group was proposed in the past (Palmer et al., 1983). The calculation scheme chosen for DIONISIO was described in detail elsewhere (Soba et al., 2013, 2014). It basically consists in adopting this simplification and restricting the balance equations to the more abundant isotopes: ^{235}U, ^{236}U, ^{238}U, ^{239}Pu, ^{240}Pu, ^{241}Pu and ^{242}Pu. Starting from reliable values of the isotopes concentrations obtained with the neutronic codes CONDOR (Villarino, 2002) and HUEMUL (Grant, 2015) in a range of irradiation conditions, empirical expressions were fitted to represent, with the higher possible accuracy, the absorption, capture and fission cross sections of these isotopes as functions of the initial enrichment in ^{235}U, the average burnup and the radial coordinate, within the approximation of one neutron energy group.

2.2.2. High burnup structure

The inhomogeneous distribution of fissile Pu isotopes that builds up for extended irradiation periods and the consequent increase of local burnup in the pellet periphery (rim zone) originate the gradual development of a new microstructure characterized by small grains and large pores as compared with those of the original material. In this region Xe is absent from the solid lattice (although it continues to be dissolved in the rest of the pellet). The porous microstructure in the pellet edge causes local changes in the mechanical and thermal properties, thus affecting the overall fuel behavior (Lassmann et al., 1995; Walker et al., 2008; Noirot et al., 2009).

A model was developed to describe the behavior and progress of porosity at local burnup values ranging from 60 to 300 MWd/kgU (Lemes, 2013). The analysis includes the interactions of different orders between open and closed pores (as in Blair, 2008; Khvostov et al., 2011), the growth of the pore radius by capturing vacancies, the evolution of the number density of pores, the overpressure within the closed pores and the inventory of fission gas dissolved in the matrix, retained in the closed pores and released to the free volume of the rod.

This model is now included as a subroutine of DIONISIO 2.0 and is interconnected with the rest of the code. The effect of porosity,

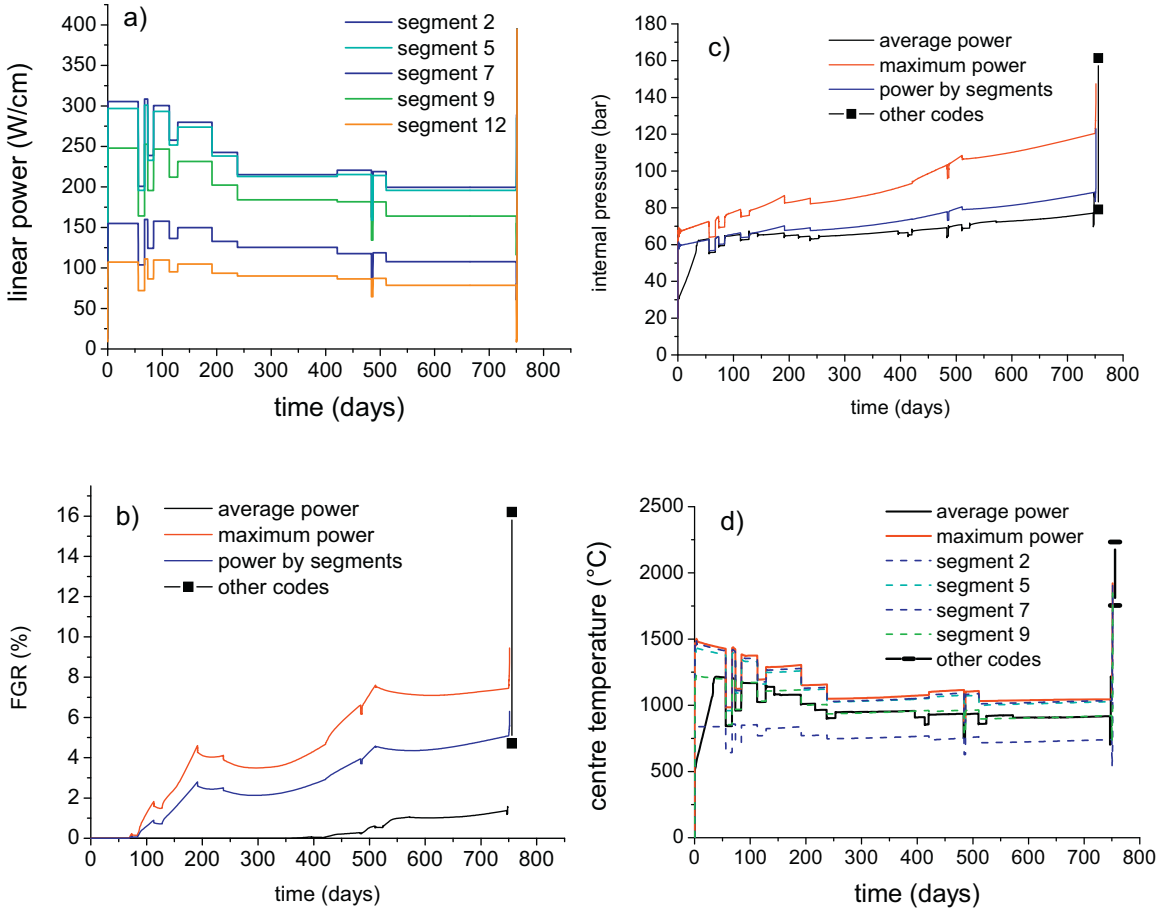

Fig. 2. (a) Experimental data of the linear power in five selected segments of the BD8 rod. (b) Fission gas release simulated under three power conditions. (c) Internal rod pressure in the same conditions as in (b). (d) Idem for the centre temperature in the whole rod; the evolution of temperature in some individual segments is also shown. In (b)–(d) the vertical lines represent the range of results at EOL of the codes participants of PRIMO.

on the one hand, is visible in the thermal conductivity of the pellet and, on the other hand, on its mechanical response, of particular interest for predicting the existence and strength of pellet-cladding mechanical interaction.

2.2.3. Concentration of Nd, Cs and Xe

Among the many fission reactions that take place during fuel irradiation, some give origin to decay chains that end in stable isotopes. How far a given fission product is found from the fission event that gave it birth is determined by its own properties in the fuel lattice as well as by those of its precursors in the fission chain.

For Nd, which exhibits a high solubility in the fuel lattice (Kleykamp, 1985), a proportionality relation can be established between its local concentration and the local burnup level (Lassmann et al., 1995). The case of Cs is somewhat different due to its high volatility and low solubility in the oxide fuel (a behavior similar to that of iodine and the noble gases) (Kleykamp, 1985) and also to the relatively long half-life of the precursor of one of the Cs isotopes (5.3 days for ^{133}Xe, precursor of ^{133}Cs Olander, 1978). For these reasons, the linear relation between local concentration and burnup shows a certain scatter. Nevertheless, the expression given in Lassmann et al. (1995) can still be accepted. On this basis, subroutines that give the Nd and Cs content as functions of the radius have been recently included in DIONISIO 2.0.

For burnup levels below the threshold for initiation of the high-bunup regime, the concentration of the stable isotopes of Xe in the fuel matrix is also proportional to burnup. Beyond the threshold, the concentration of dissolved Xe decreases exponentially with the burnup level revealing the gas depletion of the matrix and the consequent accumulation in the large pores that characterize the high-burnup microstructure. This model, which is reported in (Lassmann et al., 1995) and is in use in the TRANSURANUS code, was subjected to several separate tests (Lemes, 2013) before introduction in DIONISIO 2.0.

3. Code testing

Several experimental data reported in the IAEA and IFPE data basis were simulated with the recent version 2.0 of DIONISIO. The results presented below show the comparisons with all the items reported in the experimental data basis. Also comparisons with available results of simulations of other codes, for instance those (some 15 codes developed in different countries) which participated in international exercises of codes comparison (those of the FUMEX series IAEA, 1998; FUMEX-II, 2012; FUMEX-III, 2013), among others (van Uffelen, 2002; Sah et al., 2008) are presented.

As a first example and with the intention of showing the progress obtained with the axial partition of the rod, the conditions of the PRIMO (PWR Reference Irradiation of MOX Fuels) experiment (van Uffelen, 2002; Ott, 2009) were simulated. This program, aimed at testing the performance of eight codes from different countries, consisted in the irradiation of the single instrumented BD8 rod in the BR3 reactor during two cycles prior to being transferred to the ISABELLE 1 loop for ramping in the OSIRIS reactor. The data of the base irradiation are given as histograms of the linear power vs. time for twelve axial zones in the rod. Fig. 2a shows the experimental linear power history of five segments selected as examples, condensed to sequences of constant power steps. The final power ramp that develops in a short time interval is seen as a vertical line. The curves shown in Fig. 2b, representing the evolution of gas release, were obtained running the code in three different conditions. The red and black curves were obtained with the 1.0 code version, the red one assuming the whole rod at the maximum axial power history and the black one at the average power. In contrast, the blue curve (in between) is the result of applying the 2.0 scheme, where each of the 12 segments is subjected to its own power history and hence the threshold for gas release can be reached in some of them and not in the others. The same assumptions were applied to draw Fig. 2c for the evolution of internal pressure. The solid lines in Fig. 2d give the centre temperature obtained with the maximum and average power history, respectively. For clearness only some individual segments were selected in Fig. 2d to show the simulations with the 2.0 code version. In (b), (c) and (d) the vertical segments represent the range of results of the codes participants of the PRIMO experiment at end of life.

It is clear that the results yielded by the stepwise power profile are comprised between both limiting cases. A categorical statement about code improvement with this new architecture would require a higher refinement in the experimental data to support it (for instance, FGR determinations at several instants during irradiations) which unfortunately do not exist. Nevertheless, these results suggest that rod segmentation leads to a more realistic simulation.

A battery of experiments compiled in the IFPE data bank (OECD-NEA, in press) were simulated to test the performance of the code in its present version. The experiments, some of which reach the extended burnup range, are listed and briefly described in Table 1.

In Fig. 3 experimental data of total Uranium, Plutonium, Neodymium, Caesium and Xenon content (involving the stable isotopes) available in the tests listed in Table 1 are compared with the results of simulations performed with DIONISIO. In the five plots dotted parallel lines are drawn at both sides of the line of perfect agreement to underline the agreement between calculations

Table 1
Experiments used to validate the version 2.0 of DIONISIO.

Experiment name	No. of rods	Reactor type/fuel type	References
'IAEA_Blind'	3	PHWR, CANDU/UO_2	Sah et al. (2008)
Contact	3	PWR/UO_2	Turnbull (1998)
FUMEX I	10	PWR/UO_2	IAEA (1998)
CNEA_ MOX	2	PHWR, CANDU/MOX	Marino et al. (1996b)
PRIMO	1	PWR/MOX	Ott (2009)
AECL-bundle	4	PHWR, CANDU/UO_2	Arismescu (2000)
EFE-Ro	2	PHWR/UO_2	Paraschiv (2001)
Regate	1	PWR/UO_2	NEA-1696 (in press)
IFA507	2	BWR/UO_2	NEA-1729 (2004)
IFA535	4	BWR/UO_2	Tosi (1987)
IFA597	1	BWR/UO_2	Malén et al. (1997)
IFA534	2	PWR/UO_2	NEA-1684 (2005)
IFA 429	7	PWR/UO_2	NEA-1546 (1997)
IFA 432	5	BWR/UO_2	NEA-1488 (1996)
IFA 533.2	1	BWR/UO_2	NEA-1549 (1997)
IFA 562.1	12	BWR/UO_2	NEA-1547 (1997)
Osiris	2	PWR/UO_2	IFPE/OSIRIS (2006)
Kola3	9	WVVER/UO_2	IFPE/KOLA-3, (2011)
Riso2	16	PWR/UO_2	NEA-1502 IFPE/RISOE-II (1995)
Riso 3	15	PWR/UO_2	IFPE/RISOE III (1995)
Tribulation	19	PWR/UO_2	NEA-1536 (2002)
Hbep	79	PWR, BWR/UO_2	NEA-1510 (1990)
Gain	4	PWR, UO_2-Gd_2O_3	NEA-1625 (2002)
InterRamp	20	BWR, UO_2	Studsvik Staff (1979)
SuperRamp	44	PWR/BWR, UO_2	Djurle (1984)
Demo Ramp I/II	13	BWR, UO_2	Djurle (1981)
Over Ramp	39	PWR, UO_2	NEA-1556 (1981)
Trans Ramp	18	PWR/BWR, UO_2	Djurle (1994)
Sofit	7	WWER, UO_2	Lösönen (1996)
Br3	5	PWR, UO_2	NEA-1560 (2003)
IRDMR	7	PHWR, UO_2	NEA-1777 (2007)
USPWR 16 × 16	9	PWR, UO_2	Lyon (2005)
Spc-Re	20	PWR, UO_2	Sofer and van Swam (1997)

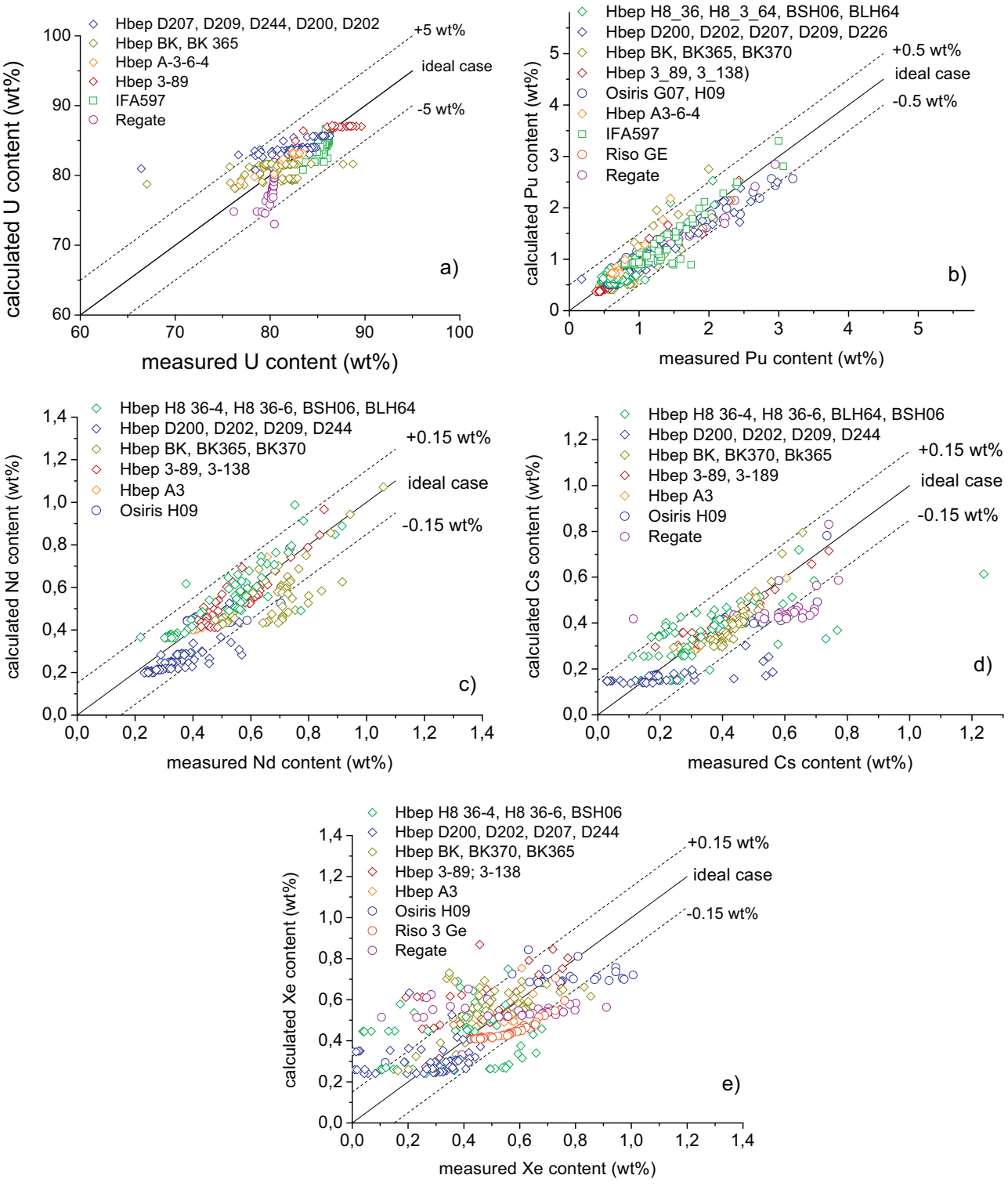

Fig. 3. Calculated vs. measured values of local concentration of (a) U, (b) Pu, (c) Nd, (d) Cs, (e) Xe.

and measurements. In particular for Pu (Fig. 3b), 97% of the nearly 270 plotted points fall within the band ±0.5 wt% at both sides of the bisector of the first quadrant. Equivalently, the mean value of the absolute difference between calculated and measured values represents 19% of the mean value of the measured data, expressing also the good quality of the approximation reached with the simulations. A similar analysis applies for the plot of the total U, Nd, Cs and Xe content where the bands are limited by lines drawn at ±5 wt% for U and at ±0.15 wt% for Nd, Cs and Xe. The dispersion observed in the plots of Nd and Cs (Fig. 3c and d) can be explained with the arguments given in Section 2.2.3. For Xe (Fig. 3e) the dispersion is probably due to the high mobility of this element so that a Xe atom can be found far from the location of the fission event that gave it birth. This explains the comparatively large amount of data falling outside the band ±0.15 wt%.

In Fig. 4 calculated and measured values of average burnup, centre temperature, FGR and internal pressure corresponding to

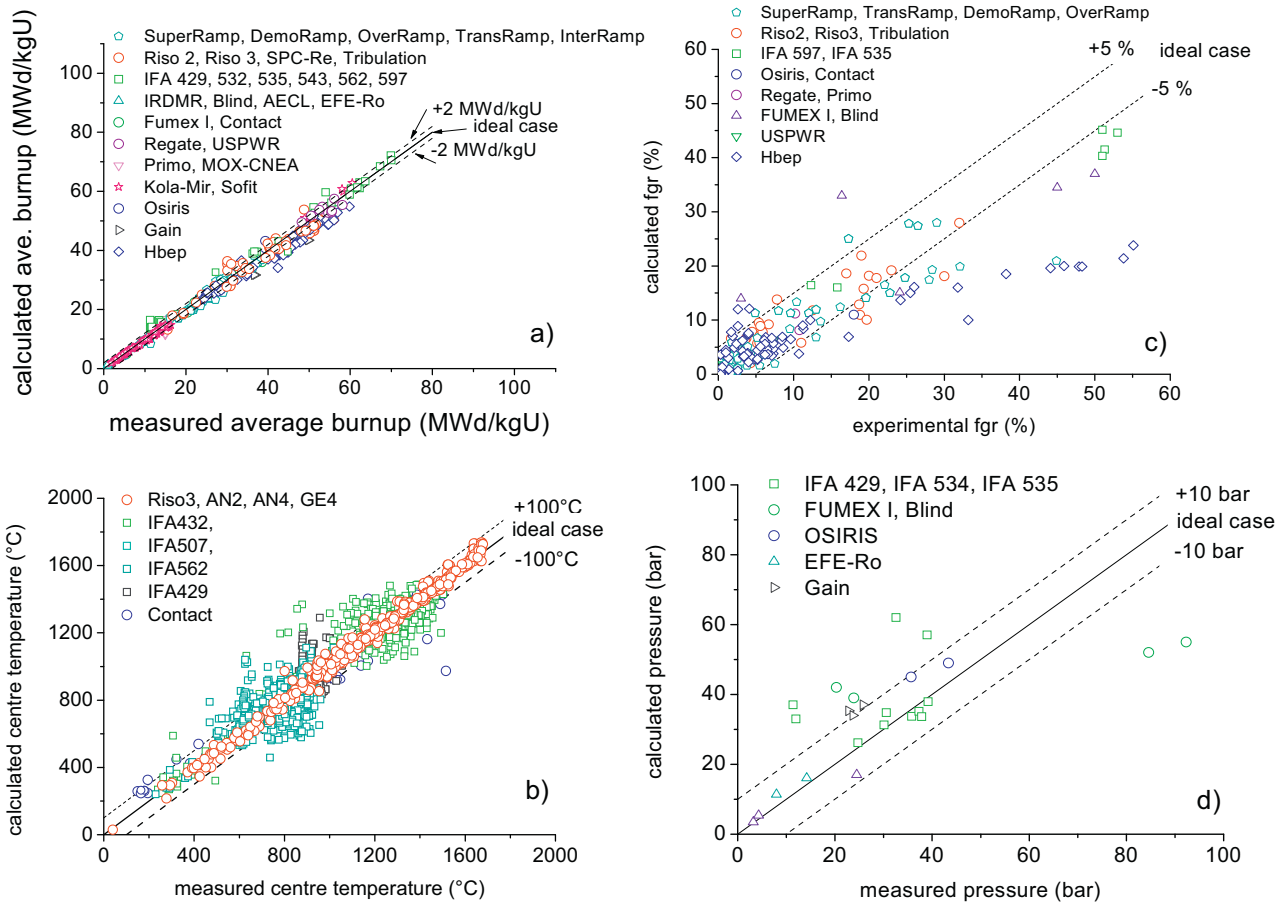

Fig. 4. Calculated vs. measured data of (a) average burnup, (b) centre temperature, (c) FGR and (d) internal pressure for experiments listed in Table 1.

experiments listed in Table 1 are compared. In particular, an excellent agreement is evidenced in Fig. 4a, where all the points representing the average burnup fall within a narrow strip of ±2 MWd/kgU around the bisecting line. In Fig. 4b the oblique lines delimit the values of the centre temperature comprised between 100 °C over and below the calculated-measured coincidence line. The major departure occurs for the IFA432 and IFA562 experiments, (particularly in the middle temperature range 600–1200 °C). This dispersion can be attributed to the difficulties in identifying the physical location of the point where the burnup measurement is performed and hence in determining its correspondence with the temperature value reported. In Fig. 4c, an acceptable agreement between calculated and measured values of FGR is seen, especially for release below 20%. Nevertheless, a trend to underprediction is recognized particularly for the values corresponding to the HBEP rods. In these experiments, abrupt final ramps were applied which most probably provoked an important release. In this respect, the DIONISIO code contains a module that gives reasonable account of gas release in isothermal processes and also in slow transients but does not possess yet the adequate subroutine to give account of fast transients. As for Fig. 4d, although the available experimental internal pressure data are comparatively scarce, the general trend is qualitatively well reproduced by the simulations.

Due to thermal expansion and mechanical restrictions, the pellet experiences a non-uniform deformation: the initially cylindrical pellet surface distorts, bending outwards, suffering a more pronounced displacement in the region of the top and bottom faces than at the central belt (Soba and Denis, 2008a). If the pellet strain is sufficiently large, it may come into contact with the cladding (PMCI), particularly in regions next to the pellet–pellet contact surfaces, giving place to a bamboo type differential deformation in the cladding evidenced by the presence of equidistant circumferential ridges. The two-dimensional structure of DIONISIO along with the model of mechanical contact included in it allows an acceptable description of the bamboo effect and the radial cladding deformation. As an example a comparison between calculated and measured determinations of strain in several rods taken from IRDMR experiments are presented in Fig. 5a. About 94% of the points are distributed within the range of ±0.2% over and below the line representing the ideal case. Even though this is a significant dispersion, representing in some cases nearly 100% of the measured value, it has to be admitted that the code gives a right guess of the order of magnitude of the strain, which experimental determinations are affected by a large relative error. As an example, the evolution of the strain in the ABS rod is presented in Fig. 5b where the upper curve corresponds to the zone of maximum strain and the lower one to the pellet mid-plane where the strain is minimal. It is seen that the general trend is correctly represented by the numerical approach of DIONISIO although a certain discrepancy between calculated and measured points is recognized. For instance, at the beginning of irradiation, the measured mid pellet strain shows an increase which is not accounted for by the code. Other discrepancies are also visible between 10 and 15 irradiation days. They are probably due to some averaging in the input power history that was performed in order to shorten the calculation time. In this respect further examination of the code and the input data need to be carried out in the near future.

In Fig. 6a calculated and measured values of ridge height corresponding to some 180 experiments from Table 1 are compared. The

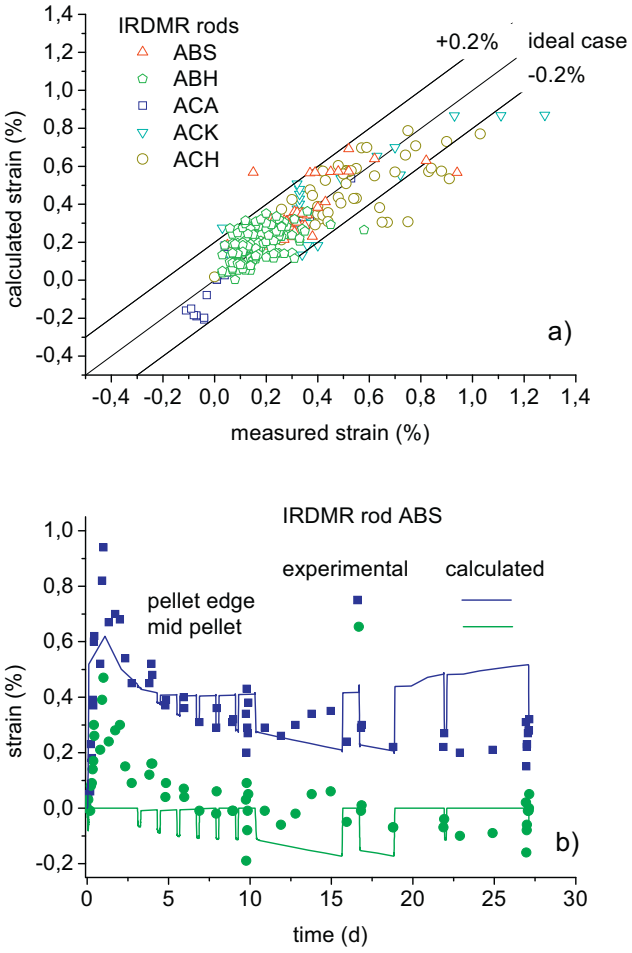

Fig. 5. (a) Comparison between measurements and the predictions of DIONISIO for several rods of the IRDMR experiment. (b) Evolution of the strain at the pellet edge and mid-plane of the ABS rod of the IRDMR experiment.

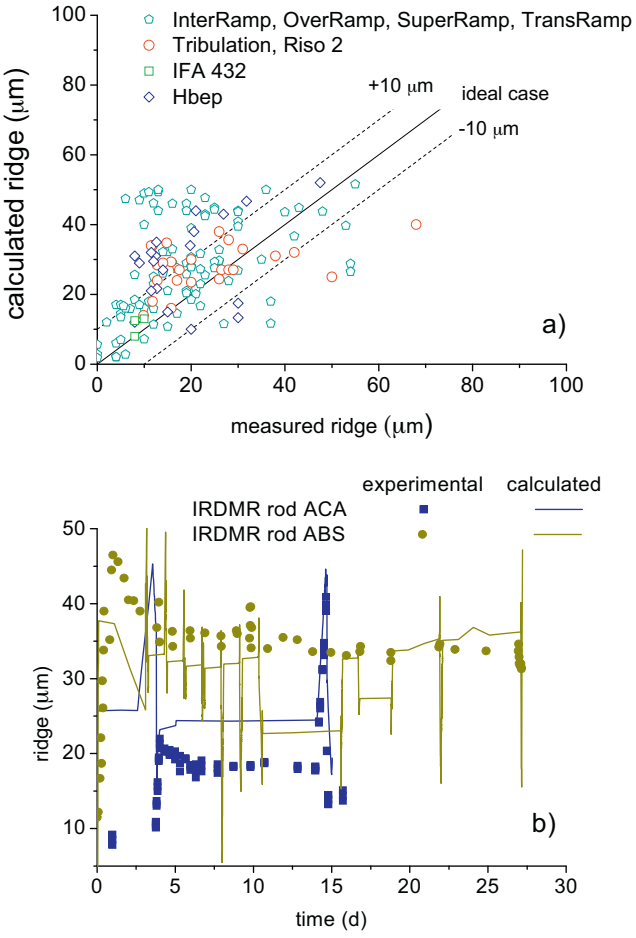

Fig. 6. (a) Calculated vs. measured values of ridge height for experiments of Table 1. (b) Evolution of the ridge height of the ACA and ABS rods of the IRDMR experiment.

rather important dispersion observed can be attributed, on the one hand, to the significant error involved in the experimental determination of the ridge height, both (measurement and error) in the range of microns. On the other hand, the algorithm of mechanical contact assumes that convergence is reached when the separation between cladding and pellet is less that a micron. But, due to the complexity involved in this algorithm, some deviations appear after several hundreds of iterations attributable to the accumulation of numerical errors. Hence, although convergence is reached, it is difficult to avoid some degree of error propagation (Soba and Denis, 2008a). Nevertheless, the ridge height is assessed within a range of $\pm 10\,\mu m$ in about 80% of the cases of an extensive battery of experiments. There exists a tendency to over-prediction in the calculated data which can be also attributed to the contact algorithm used in the code. The algorithm used in DIONISIO, that assumes non-sliding contact conditions, is explained in detail in (Soba and Denis, 2008a). This type of solid–solid interaction is the more adequate election for the two-dimensional domain with axial symmetry considered in this work but is probably the cause of some overestimation of the contact stress and cladding deformation.

Fig. 6b shows the evolution of the ridge in two different rods (ACA and ABS) of the IRDMR experiments, which are compared with the predictions of DIONISIO. A good qualitative agreement is observed in these examples too; the difference between calculations and measurements is not higher than $10\,\mu m$ even in the worse portions of the experiments.

Given the results presented in Figs. 5 and 6, it can be assessed that the simulations with DIONISIO provide a good picture of the strains, stresses and pellet-cladding mechanical interactions that take place in a particular rod during a power history.

4. Conclusions

The architecture of the present version of DIONISIO provides a more realistic simulation of the fuel rod behavior since each axial section can be modeled starting from the local conditions of linear power and coolant temperature. Due to the non-uniformity of the conditions to which the different portions of fuel rod are subjected during operation, several phenomena can start at (or take place only in) the central part of the bar and begin much later (or never happen) at its ends. The release of fission gases and the pellet-cladding mechanical contact are just two examples of phenomena with this differential behavior. The previous version of DIONISIO (1.0) assumed a uniform power in the whole rod length. The choice of the average linear power for this purpose leads to under-prediction of the amount of gas released or to over-prediction of the time for initiation of release, and vice versa if the simulation is carried out assuming the whole rod at the maximum power.

As stated in Section 2.1, in the new code version the axial discretization of the rod can be refined even to give an individual description of each pellet. Nevertheless, this would imply a large computational cost and require code parallelization, a work which is currently in progress.

The results presented in this paper reveal that, beyond certain degree of departure between measurements and calculations, the

code performance is correct, giving an adequate overall description of the relevant parameters of the fuel rod, required for the design and analysis of behavior in operation.

A wide range of data was used to make the comparisons, spanning a variety of fuel designs and operation conditions. Data obtained in experiments performed with standard fuel rods of the PWR, BWR, PHWR, CANDU and WWER types were used. The controlled experiments correspond to high, media or low burnup. Some of them were carried out on rods irradiated in commercial reactors and then instrumented to record particular behavior features.

With the improvements recently introduced, involving also subroutines for the physical and chemical properties of the fuel material in the high burnup range, the code DIONISIO in its version 2.0 evidences a good performance in the many simulations carried out. Given the complexity of the experiments and the number of physical and chemical parameters involved, the degree of dispersion between calculations and measurements does not invalidate considering the DIONISIO 2.0 code as an acceptable prediction tool even for average burnup levels as high as 60 MWd/kgU.

References

Arismescu, V., 2000. NEA-1596 IFPE/AECL-BUNDLE. Chalk River, ON.

Baurens, B., Sercombe, J., Riglet-Martial, C., Desgranges, L., Trotignon, L., Maugis, P., 2014. 3D thermo-chemical-mechanical simulation of power ramps with ALCYONE fuel code. J. Nucl. Mater. 452, 578–594.

Blair, P., 2008. Modelling of Fission Gas Behaviour in High Burnup Nuclear Fuel. École Polytechnique Federale de Lausanne, Swizerland (Ph.D. Thesis).

Denis, A., Piotrkowski, R., 1996. Simulation of isothermal fission gas release. J. Nucl. Mater. 229, 149–154.

Denis, A., Piotrkowski, R., 1997. A fission gas release model. In: Water Reactor Fuel Element Modeling at High Burnup and Experimental Support, IAEA-TECDOC-957., pp. 455–465.

Denis, A., Soba, A., 2003. Simulation of pellet-cladding thermomechanical interaction and fission gas release. J. Nucl. Eng. Des. 223, 211–229.

Djurle, S., 1981. Final Report of the STUDSVIK DEMO-RAMP I Project, STUDSVIK-STDRI-18 (1983); STUDSVIK-STDRII-13; THE STUDSVIK DEMO-RAMP II Project. Final Report.

Djurle, S., 1994. STUDSVIK-STTRI-10 Final Report of the TRANS-RAMP I Project (1985); NEA-1648 IFPE/TRANS-RAMP-I II and IV (2003); STUDSVIK/SLTRIV-25.

Djurle, Seved, 1984. Final Report of the Super-ramp Project. Studsvik.

Fuel Modelling at Extended Burnup (FUMEX-II), 2012. IAEA TECDOC 1687.

FUMEX-III, 2013. Improvement of computer codes used for fuel behaviour simulation (FUMEX-III). In: IAEA-TECDOC-1697.

Geelhood, K., Luscher, W., Beyer, C., Flanagan, M., 2011. FRAPCON-3.4: a computer code for the calculation of steady-state thermal-mechanical behavior of oxide fuel rods for high burnup. In: NUREG/CR-7022 (1).

Grant, C., Manual del Sistema HUEMUL, Version 4. Informe Interno CNEA, MCO-06-REC-1. code (2015).

IAEA-TECDOC-998, Report of the Co-ordinated Programme on Fuel Modelling at Extended Burnup-FUMEX, IAEA 1998.

Turnbull, J.A., 1998. IFPE/CONTACT. Rev.1., Database for CONTACT experiments irradiated at CEA Grenoble.

IFPE/KOLA. IFPE/KOLA-3-MIR-RAMP, NEA-1766/02, 2011.

IFPE/OSIRIS, NEA-1622/04, 2006.

IFPE/RISOE III, NEA-1493/17, 1995.

Khvostov, G., Mikityuk, K., Zimmermann, M., 2011. A model for fission gas release and gaseous swelling for the uranium dioxide fuel coupled with the FALCON code. Nucl. Eng. Des. 241, 2983–3007.

Kleykamp, H., 1985. The chemical state of the fission products in oxide fuels. J. Nucl. Mater. 131, 221–246.

Lassmann, K., Walker, C., van de Laar, J., Lindström, F., 1995. Modeling the high burnup UO2 structure in LWR fuel. J. Nucl. Mater. 226, 1–8.

Lassmann, K., Schubert, A., van de Laar, J., Vennix, C., 2003. Recent developments of the TRANSURANUS code with emphasis on high burnup phenomena. Int. Conf. Nucl. Fuel Today Tomorrow.

Lassmann, K., 1992. TRANSURANUS: a fuel rod analysis code ready for use. J. Nucl. Mater. 188, 295–302.

Lemes, M., 2013. Estudio analítico y numérico de los efectos de la irradiación hasta alto quemado en combustibles de reactores de potencia. Instituto Sabato, University of San Martín, Argentina (Master Thesis).

Linet, B., Suo, X., 1993. The METEOR/TOUTATIS code A 2D/3D code for fuel behaviour simulation. In: Canadian Nuclear Society/American Nuclear Society Fourth International Conference on Simulation Methods in Nuclear Engineering, Canada, p. 2v.

Lösönen, P., 1996. Verification of TRANSURANUS code against temperature data from WWER type test tie1 rods from SOFIT experiments. In: IAEA/OECD Data Base Training Meeting, Halden, Norway.

Lyon, W.F., 2005. US-PWR 16x16 LTA Extended Burnup Demonstration Program Summary File.

Malén, K., Micski, A., Schrire, D., Nilsson, B., 1997. PIE of High Burnup BWR Fuel Rod IFA-597.3 (Rod8). Studsvik Nuclear AB SwedenHRP-356/U.

Marino, A.C., Savino, E.J., Harriague, S., 1996a. BACO (Barra Combustible) code version 2.20: a thermo-mechanical description of a nuclear fuel rod. J. Nucl. Mater. 229 (2), 155–168.

Marino, A., Pérez, E., Adelfang, P., 1996b. Irradiation of Argentine (U,Pu)O2 MOX fuels. Postirradiation results and experimental analysis with the BACO code. J. Nucl. Mater. 229, 169–186.

MATPRO Version 11, 1979. Handbook of materials properties for use in the analysis of light water reactor fuel behavior. In: NUREG/CR-0497, TREE-1280.

MPI: A Message-Passing Interface Standard, Version 3.1 (2015) Ed: University of Tennessee.

NEA-1488, 1996. NEA-1488 IFPE/IFA-432.

NEA-1502 IFPE/RISOE-II, 1995. Fuel Performance Data from Transient Fission Gas Release.

NEA-1510. IFPE/HBEP-3 REV.1, High Burnup Effects Programme. Final Report, DOE/NE/34046-1 [HBEP-61(3P27)], 1990.

NEA-1536. IFPE/TRIBULATION R1, 2002.

NEA-1546, 1997. IFPE/IFA-429.

NEA-1547, 1997. IFPE/IFA-562.1.

NEA-1549, 1997. IFPE/IFA-533.2.

NEA-1556 IFPE/OVER-RAMP (1997), 1981. The studsvik over-ramp project final report. In: STUDSVIK-STOR-37.

NEA-1560, 2003. IFPE/BR3-HBFRHCP.

NEA-1625. IFPE/GAIN, 2002.

NEA-1684, 2005. IFPE/IFA-534.14REV.1.

NEA-1696. IFPE/REGATE L10.3.

NEA-1729, 2004. IFPE/IFA-507-TF3-TF5.

NEA-1777, 2007. IFPE/CANDU-IRDMR.

Noirot, J., Aubrun, I., Desgranges, L., Hanifi, K., Lamontagne, J., Pasquet, B., Valot, C., Blanpain, P., 2009. High burnup changes in UO2 fuels. Nucl. Eng. Technol. 41 (2), 155–162.

OECD-NEA, ⟨http://www.oecd-nea.org/science/fuel/ifpelst.html⟩.

Olander, D., 1978. Fundamental Aspects of Nuclear Reactor Fuel Elements. University of California, Berkeley, USA.

OpenMp Technical Report 3 on OpenMP 4.0 enhancements, (2014) Ed: www.openmp.org

Ott, L.J., 2009. Mixed-oxide (MOX) fuel performance benchmark. In: Summary of the Results for the PRIMO MOX rod BD8. NEA No. 6291.

Palmer, I.D., Hesketh, K.W., Jackson, P.A., 1983. In: Gittus, J. (Ed.), Water Reactor Fuel Element Performance Computer Modelling. Applied Science Publishers, UK, pp. 321–335.

Palmer, I., Rossiter, G., White, R., 2000. Development and validation of the ENIGMA code for MOX fuel performance modelling. In: MOX Fuel Cycle Technologies for Medium and Long Term Deployment, IAEA/OECD Symposium, Vienna, p. 271.

Paraschiv, M.C., 2001. Romanian irradiation tests, OECD/IAEA. In: IFPE Database.

Sah, D.N., Viswanathan, U.K., Viswanadham, C.S., Unnikrishnan, K., Rath, B.N., 2008. Blind prediction exercise on modelling of PHWR fuel at extended burnup. J. Nucl. Mater. 383, 144–149.

Soba, A., Denis, A., 2006. Simulation of PHWR fuel rods behavior with the code DIONISIO 1.0. In: Technical Meeting on Pressurised Heavy Water Reactor (PHWR) Fuel Modelling, Mumbai, India.

Soba, A., Denis, A., 2008a. Simulation with Dionisio 1.0 of thermal and mechanical pellet-cladding interaction in nuclear fuel rods. J. Nucl. Mater. 374, 32–43.

Soba, A., Denis, A., 2008b. Model of fracture for the Zry cladding of nuclear fuel rods included in the code DIONISIO 1.0. Nucl. Eng. Des. 238, 3292–3298.

Soba, A., Denis, A., Romero, L., Villarino, E., Sardella, F., 2013. A high burnup model developed for the DIONISIO code. J. Nucl. Mater. 433, 160–166.

Soba, A., Lemes, M., González, M.E., Denis, A., Romero, L., 2014. Simulation of the behaviour of nuclear fuel under high burnup conditions. Ann. Nucl. Energy 70, 147–156.

Soba, A., 2007. Simulación del comportamiento termomecánico de una barra combustible en operación. University of Buenos Aires, Ph.D. Thesis.

Sofer, G., van Swam, L., 1997. SPC-re-ginna: Annular-Pellet Barrier-Clad Fuel Assemblies at the R.E. Ginna PWR: Hotcell Examinations EP 80-17, Final Report Volume 1.

Studsvik, Staff, 1979. Final Report of the Inter-ramp Project. Studsvik Staff.

Suzuki, M., Saitou, H., Udagawa, Y., Nagase, F., Light Water Reactor Fuel Analysis Code FEMAXI-7, Model and Structure, JAEA-Data/Code 2013-005, Suzuki.

Tosi, V., 1987. The effect of pressurisation on fission gas release in high burnup BWR-type fuel rods (IFA-535.5-6), HWR-198. In: NEA-1548/01.

van Uffelen, P., 2002. PRIMO, PWR Reference Irradiation of MOX Fuels, Data of a Ramped MOX Fuel Rod, SCK-CEN. Mol, Belgium.

Villarino, E., October 2002. CONDOR Calculation Package. In: PHYSOR 2002. PHYSOR, Seoul, Korea, pp. 7–10.

Walker, C., Bremier, S., Portier, S., Hasnaoui, R., 2008. SIMS analysis of Xe and Kr in a high burn-up UO2 nuclear fuel. Microsc. Microanal. 14 (2), 1092–1093.

Williamson, R., Hales, J., Novascone, S., Tonks, M., Gaston, D., Permann, C., Andrs, D., Martineau, R., 2012. Multidimensional multiphysics simulation of nuclear fuel behavior. J. Nucl. Mater. 423, 149–163.

Zangari, A., Montgomery, R., 2004. Fuel analysis and licensing code: FALCON MOD01. In: Volume 2: User's Manual Technical Report EPRI 1011308.